Check for updates

Fasting-induced activity changes in MC3R neurons of the paraventricular nucleus of the thalamus

Robert A Chesters[1,*], Jiajie Zhu[1,3,*], Bethany M Coull[1,3], David Baidoe-Ansah[1,3], Lea Baumer[1], Lydia Palm[1], Niklas Klinghammer[1], Seve Chen[1] , Anneke Hahm[1], Selma Yagoub[1], Lídia Cantacorps[1,2], Daniel Bernardi[1], Katrin Ritter[1], Rachel N Lippert[1,2,3]

The brain controls energy homeostasis by regulating food intake through signaling within the melanocortin system. Whilst we understand the role of the hypothalamus within this system, how extra-hypothalamic brain regions are involved in controlling energy balance remains unclear. Here we show that the melanocortin 3 receptor (MC3R) is expressed in the paraventricular nucleus of the thalamus (PVT). We tested whether fasting would change the activity of MC3R neurons in this region by assessing the levels of c-Fos and pCREB as neuronal activity markers. We determined that overnight fasting causes a significant reduction in pCREB levels within PVT-MC3R neurons. We then questioned whether perturbation of MC3R signaling, during fasting, would result in altered refeeding. Using chemogenetic approaches, we show that modulation of MC3R activity, during the fasting period, does not impact body weight regain or total food intake in the refeeding period. However, we did observe significant differences in the pattern of feeding-related behavior. These findings suggest that the PVT is a region where MC3R neurons respond to energy deprivation and modulate refeeding behavior.

Introduction

The progression of obesity, diabetes, and other metabolic disorders in our society is occurring at an alarming speed, and there is a great need to understand the underlying physiological changes that are occurring. Current preclinical animal models used to study obesity rely on either genetic models or, more frequently, long-term exposure to unhealthy diets across weeks/months (Lutz & Woods, 2012; Suleiman et al, 2020; de Moura E Dias et al, 2021). These studies highlight that it is the gradual accumulation of small behavioral, physiological, and molecular changes that shift energy balance in a positive direction, leading to an increased likelihood of obesity (Schwartz et al, 2017). The control of energy balance is predominately regulated through changes in the brain (Cone, 1999, 2005; Ellacott & Cone, 2004; Dietrich & Horvath, 2013).

The primary regulating system of energy balance in the brain is the central melanocortin system (Cone, 2005). Agouti-related peptide (AgRP) and proopiomelanocortin (POMC) neurons reside in the arcuate nucleus (ARC) of the hypothalamus and send projections to brain regions expressing melanocortin receptors to mediate aspects of energy balance. Almost all studies related to fasting or feeding responses have focused on this system and its activity directly within the hypothalamus.

A number of recent studies centered on this system have focused on the rapid neuronal changes that occur in response to immediate feeding-related actions such as the sight, smell and taste of food, immediately after a fasting period (Chen et al, 2015; Chen & Knight, 2016; Brandt et al, 2018; Alhadeff et al, 2019; Li et al, 2019). The subcellular mechanisms responsible for these changes are complex and are likely mediated by a number of intracellular signaling pathways. These are actively under investigation and are specifically being studied in AgRP neurons (Kong et al, 2016; Bruning & Fenselau, 2023; Grzelka et al, 2023). Moreover, how changes within AgRP neurons affect downstream neuronal networks and subsequent feeding behavior, be it food consumption or cessation of feeding, is an active area of research. Sayar-Atasoy and colleagues recently reported that AgRP neurons integrate information about circadian feeding with current metabolic needs to determine future feeding times (Sayar-Atasoy et al, 2024). This is relevant to studies of energy deprivation in rodents, as many studies use fasting paradigms from periods of 9 h up to 48 h (Wu et al, 2014; Steculorum et al, 2016; Gui et al, 2023), with the most widely used paradigm involving a 16-h fast with an onset at the beginning of the dark phase. Whereas an assessment of the effects of fasting (across different timespans) is known in peripheral tissues (liver and muscle) (Kinouchi et al, 2018), an assessment of the effects of fasting, across different Zeitgeber (ZT) timespans, on extra-hypothalamic neuronal circuits involved in the energy balance is lacking and was the primary goal of this study.

[1]Department of Neurocircuit Development and Function, German Institute of Human Nutrition, Nuthetal, Germany   [2]German Center for Diabetes Research (DZD), München-Neuherberg, Germany   [3]NeuroCure Cluster of Excellence, Charité-Universitätsmedizin, Berlin, Germany

Correspondence: rachel.lippert@dife.de
*Robert A Chesters and Jiajie Zhu contributed equally to this work

Studies of energy deprivation through fasting have assessed the expression of the immediate early gene, c-Fos, as a marker for increased neuronal activity and have shown increased levels in AgRP neurons within the ARC (Steculorum et al, 2016; Gui et al, 2023). However, studies assessing neuronal responses to fasting, in extra-hypothalamic brain regions are less prevalent, especially in regions known to have direct connectivity to the AgRP and POMC neurons of the ARC. Those that do exist have investigated the potential intersection of energy state and food intake, food choice and food reward (Zhang & van den Pol, 2017; Li et al, 2019; Mazzone et al, 2020).

The melanocortin 4 receptor has been the focus in studies of the hypothalamic AgRP and POMC neuronal projections (Atasoy et al, 2012), but it is not the only centrally expressed melanocortin receptor. The melanocortin 3 receptor (MC3R) is also expressed in a number of brain regions, independent of the melanocortin 4 receptor, suggestive of a different role for this centrally expressed melanocortin receptor (Roselli-Rehfuss et al, 1993). The MC3R acts as a central rheostat, coordinating not only aspects of energy excess but also energy deprivation (Ghamari-Langroudi et al, 2018). MC3R deficient animals show both a defective fasting response, highlighted by decreased refeeding upon food presentation, and changes to c-Fos activation in the ARC and in reward circuits (Renquist et al, 2012; Girardet et al, 2017; Ghamari-Langroudi et al, 2018; Gui et al, 2023).

Deficiency of the MC3R results in altered body composition, mild obesity, alterations to feeding behaviors such as food anticipatory activity, and changes to reward-related intake (Butler et al, 2000, 2017; Begriche et al, 2012; Lippert et al, 2014). Alterations in feeding behaviors have also been identified in humans with MC3R mutations (Obregon et al, 2010; Aris et al, 2016). Furthermore, recent studies have uncovered a role for the MC3R in a number of other, non-homeostatic aspects of energy balance and behavior, such as reward-based or stress-induced feeding (Pandit et al, 2015, 2016; Roseberry et al, 2015; Yen & Roseberry, 2015; Pei et al, 2019; West et al, 2019; Sweeney et al, 2021; Cho et al, 2023). Many of these actions have been targeted to extra-hypothalamic regions expressing the MC3R, highlighted by the recently updated neuroanatomical assessment of MC3R in the brain (Bedenbaugh et al, 2022).

In the context of extra-hypothalamic regions involved in food intake, a pivotal study assessing AgRP projection stimulation and food intake highlighted additional target regions, including the paraventricular nucleus of the thalamus (PVT) (Betley et al, 2013). Optogenetic activation of these AgRP neuronal projections to the PVT led to increased feeding (Betley et al, 2013). Moreover, AgRP neuronal projections to the PVT can facilitate food-seeking behaviors in the fasted condition (Wang et al, 2021). Recent interest has increased in probing how the PVT may interact with metabolic circuits (Kirouac, 2015; Millan et al, 2017; Petrovich, 2021). The PVT is a midline structure that receives inputs from multiple brain regions (Kirouac, 2015; Iglesias & Flagel, 2021), and is a relevant relay center involved in feeding behavior (Zhang & van den Pol, 2017; Cheng et al, 2018; Horio & Liberles, 2021), reward (Parsons et al, 2007; Clark et al, 2017; Do-Monte et al, 2017; Meffre et al, 2019; Otis et al, 2019; Iglesias & Flagel, 2021), fear (Li et al, 2014; Penzo et al, 2015), stress (Dong et al, 2020; Gao et al, 2020; Rowson & Pleil, 2021), and anxiety processing (Cho et al, 2023).

To identify PVT neurons mediating aspects of energy balance, we systematically characterized the neuroanatomical distribution of

the MC3R within the thalamus and showed that it is highly expressed throughout the PVT. We also analyzed how this nucleus responds to two fasting conditions, overnight and daytime, by quantifying immediate early gene protein expression and phosphorylation of a known signaling mediator, which we hypothesized would be reduced within MC3R-positive neurons. Furthermore, we questioned whether perturbation of MC3R activity during fasting would result in changes to refeeding behaviors in a mouse model with Designer Receptors Exclusively Activated by Designer Drug (DREADD)-mediated activation or inhibition. This work shows the effects of time of day and energy state on PVT-MC3R neurons and highlights behaviors related to feeding which are mediated by MC3R activity in both male and female animals.

Results

MC3R robustly expressed in the thalamus, with predominant expression in the PVT

To investigate the expression of the MC3R in the thalamus, we used the MC3R-GFP mouse model where GFP is expressed under the direct control of the MC3R promoter. Neurons expressing MC3R were seen in the central medial nucleus (CM), the central lateral nucleus (CL), the intermediodorsal nucleus (IMD), and the PVT in both male and female mice (see Fig 1A–D). Quantification of individual neurons shows a predominant expression in the PVT (see Fig 1D). As the anterior to posterior axis of the PVT was recently shown to have functionally distinct cell types (Gao et al, 2020), we subsequently subdivided quantification of MC3R neurons across the anterior (aPVT), mid (mPVT), and posterior (pPVT) (see Fig 1A–C and E). We found the greatest number of MC3R neurons in the pPVT.

Time of day influences the effect of fasting on PVT activation

After confirming the expression of the MC3R across the anterior to posterior axis of the PVT, we next sought to understand how neurons in the PVT respond to energy deprivation. Neuronal activity, and markers thereof, are used to assess steady-state chronic activation of neuronal circuits (Bartel et al, 1989; Sheng & Greenberg, 1990; Ginty et al, 1992; Ji & Rupp, 1997; Wu et al, 2001). Here we first assessed PVT activation in the context of fasting. In the field, a wide range of fasting times are used and up to 24–48 h of fasting has been shown to activate neuronal circuits (Wu et al, 2014; Girardet et al, 2017; Horio & Liberles, 2021; Cho et al, 2023; Gui et al, 2023). However, despite their tolerability, longer periods of fasting are associated with a physiological response more similar to starvation than normal physiological feeding (Moro & Magnan, 2021). Here we investigated two fasting periods, subjecting mice to either an overnight fast of 16 h (ZT12-ZT4) or a daytime fast (ZT4-ZT20, see Fig 2A), time locked to the peak night phase of normal food intake to replicate the previous c-Fos activation studies (Steculorum et al, 2016; Chen et al, 2023). In both time periods, fasted males and females lost weight, compared with their fed counterparts (see Figs 2B and S1B). Using the neuronal activity marker c-Fos, and with the exception of the pPVT in the male
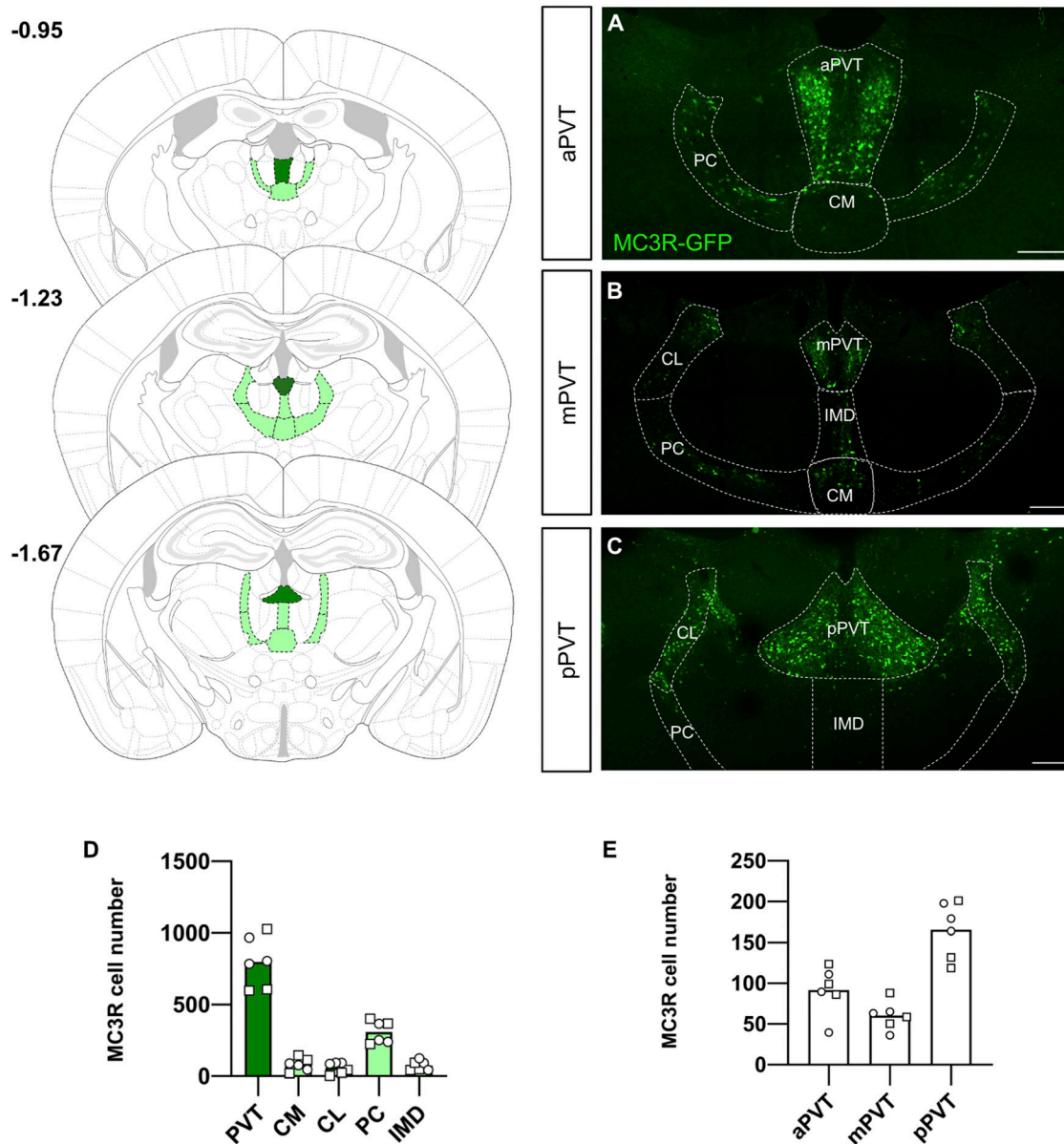
Figure 1. Neuroanatomical distribution of melanocortin 3 receptor (MC3R) neurons in the thalamus.
(A, B, C) Left panel shows representative images of thalamic nuclei at −0.95 (A), −1.23 (B), and −1.67 (C) relative to Bregma. **(D)** Quantification of MC3R neuronal number in the five most populated thalamic nuclei: paraventricular nucleus of the thalamus (PVT), central medial (CM), central lateral (CL), paracentral (PC), and intermediodorsal (IMD). **(E)** Quantification of MC3R neurons in different regions of the PVT: anterior (aPVT), mid (mPVT), and posterior (pPVT). Male data points are represented as circles and female data points as squares. Scale bars in (A, B, C) are 200 µm.
Source data are available for this figure.

daytime fasting experiment (Fig S1G–I, P = 0.014), in general, we did not see any differences across the anterior to posterior axis of the PVT between fed and fasted groups, neither in males or females, either in the daytime or overnight fast (see Figs 2C–P and S1C–P).

pCREB cell density is decreased in response to fasting

Whereas c-Fos is a primary marker of neuronal activity, studies suggest that c-Fos expression in general is the result of multiple waves of neuronal activity and may not reflect more acute

activation of neurons (Anisimova et al, 2023 Preprint). Thus, we opted to further probe upstream signaling pathways that would be activated upon stimulation of intracellular signaling cascades related to changes in energy state. We used immunolabeling of the phosphorylated form of the cyclic AMP response element binding protein (pCREB). CREB is an immediate upstream marker of c-Fos and was recently used to indicate significant changes to overall PVT activity (Kato et al, 2019). Analysis of pCREB immunolabeling showed a significant reduction in cellular density in the mPVT and pPVT in females in both the daytime (see Fig 3A–G) and the overnight (see
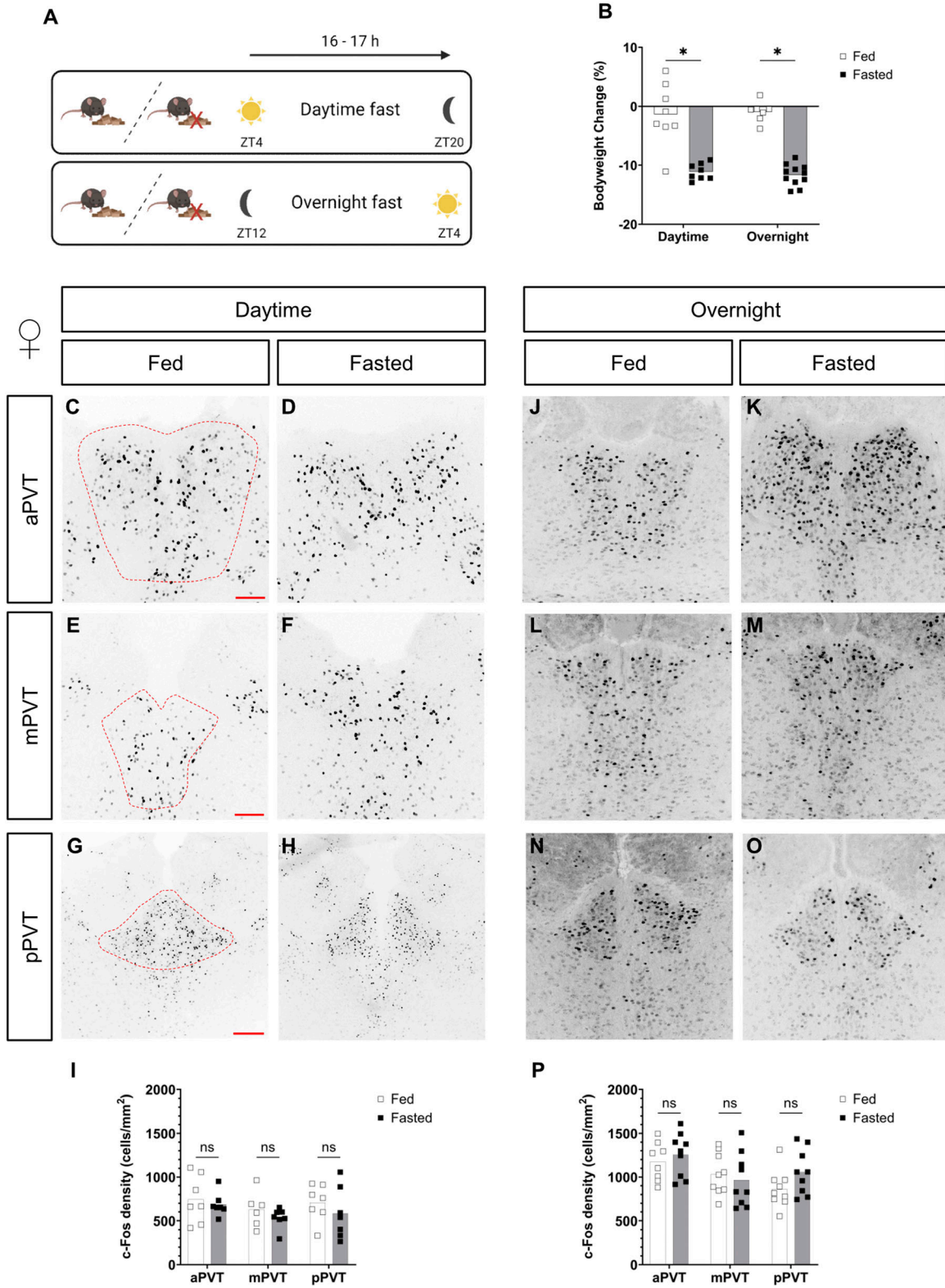
Figure 2. Comparison of c-Fos cell density, in the paraventricular nucleus of the thalamus (PVT), of fed versus fasted female mice.
(A) Experimental paradigm. Zeitgeber (ZT). **(B)** Percentage of body weight change at the start and end of the fasting period. **(C, D, E, F, G, H, I, J, K, L, M, N, O)** Representative images of c-Fos–positive cells in the anterior PVT (aPVT), mid PVT (mPVT), and posterior PVT (pPVT). **(C, E, G)** The red dashed outline in (C, E, G) represents regions of interest drawn around the PVT for analysis. **(I, P)** Quantification of c-Fos cell density in daytime (I) and overnight (P) fasting experiments. **(G)** Scale bars in (C, E) are 100 and 200 μm in (G). Unpaired Welch t tests: *$P \leq 0.05$, ns, non-significant.
Source data are available for this figure.

Fig 3H–N) fasts. In males, there was no difference between groups, in the daytime fast (see Fig S2A–G). However, decreases in pCREB were seen in the overnight fast, and were significant in the pPVT (see Fig S2H–N). These changes indicate a more pronounced effect of fasting in females.

MC3R neuronal activity markers decrease in the fasted state

To determine the direct effect of fasting on MC3R neuronal activity, colocalization of MC3R with c-Fos and pCREB immunolabeling was assessed using the MC3R-GFP mouse model. In line with the overall lack of effect on c-Fos activation in the PVT, and with the exception of the pPVT in daytime fasted female mice (Fig S3E–G, $P = 0.04$), in general, the colocalization of c-Fos with MC3R-GFP was no different between fed and fasted females (see Fig S3) or males (see Fig S4) in either the daytime or overnight fasts.

However, contrary to the lack of difference in the MC3R-c-Fos co-labeling, levels of MC3R-pCREB–positive neurons were significantly reduced in the PVT of females exposed to an overnight fast (see Fig 4H–N) but not in those exposed to a daytime fast (see Fig 4A–G). In males, there was no significant difference between groups, in MC3R-pCREB–positive cells, in either the daytime or overnight fasts (see Fig S5).

AgRP neuropeptide levels and projections are not changed in the PVT in response to fasting

Recent studies suggest that in response to changes in energy state, the synaptic contacts or neuronal projections of AgRP neurons may be altered (Wei et al, 2015; Grzelka et al, 2023). To determine if changes in activity were linked to gross anatomical reductions in AgRP projection density, these were assessed in the PVT of fed and fasted, male and female mice. No group-level differences were observed in AgRP projections, in either male or female mice, in both the daytime and overnight fasts (see Figs S6 and S7). This suggests that changes to pCREB activation in the PVT are not because of significant alterations in AgRP projections to the region.

Modulation of MC3R activity during fasting does not alter cumulative refeeding and body weight response

Reduced activity of MC3R neurons in response to a fast was shown at the level of pCREB cellular density in the PVT specifically in response to the overnight fasting paradigm. Here we aimed to determine how the direct activation state of MC3R cells may regulate the fasting response. Using a chemogenetic approach, we tested if heightened MC3R activity during the fasting period would result in suppression of body weight loss during fasting or in an alteration in refeeding. To address this question MC3R-Cre mice were crossed to floxed-hM3DGq mice to result in offspring with the activating DREADD receptor, hM3DGq, expressed in all MC3R cells in the body (see Fig S8). The fasting experiment (see Fig 5A) was performed with clozapine-*n*-oxide (CNO) application and subsequent activation of all MC3R cells. As a single injection of CNO can exert a biological effect up to 6–10 h, mice were injected twice across the dark period (Alexander et al, 2009; Wess et al, 2013; Biglari et al, 2021). No difference in body

weight loss during fasting was detected in either females or males given CNO versus saline (see Figs 5 and S9). Furthermore, there was no difference in refeeding in the acute (1–12 h) or sustained (1–3 d) period after fasting (see Fig 5D and E). This was accompanied by no difference in the body weight regain during the refeeding period (see Fig 5C).

In a complementary experiment aiming to determine if MC3R inactivation during fasting may result in a reduced feeding re-bound after fasting, the inhibitory DREADD receptor, hM4DGi, was expressed in all MC3R-positive cells. As MC3R knockout animals are known to have a defective response to fasting (Renquist et al, 2012), we tested whether acute inhibition of MC3R cells during the fasting period would mimic the phenotype of the whole-body knockout animal to determine if the acute activity change in these neurons is necessary for refeeding responses. To do this, MC3R-Cre animals were crossed with floxed-hM4DGi animals, to result in hM4DGi expression localized to all MC3R-positive cells. Mice received acute injections of CNO at two timepoints across the fasting period to ensure sufficient inhibition (see Fig 6A). At the start of the light phase, mice were exposed to food, and their refeeding response was recorded. We did not find a difference in body weight loss because of fasting, in either females or males given CNO versus saline (see Figs 6A and S10A). There were also no differences in food intake and body weight measurements, in CNO versus saline groups (see Figs 6B–D and S10B–D).

Modulation of MC3R neurons during fasting changes behavioral patterns during initial refeeding

Although there were no differences in body weight or food intake across the hours and days post-fasting, we did see a significant difference in the behavior of the mice during the first hour of refeeding. We established an analysis pipeline using DeepLabCut (DLC) and Simple Behavior Analysis (SimBA) to assess the behavior of the MC3R; hM3DGq and MC3R; hM4DGi mice (see Fig 7A and B). Specifically, we measured the time spent in different areas of the home cage, including time spent at the newly re-stocked food hopper. In MC3R; hM3DGq male and female animals (grouped together), CNO-treated mice spent significantly more time interacting with the food hopper (and the tip of the water bottle) than saline-treated mice (Fig 7C and D), whereas there was no significant difference between treatment groups in the MC3R and hM4DGi mice. Additional assessment of the time spent in the residual zone (Fig S11), consumption zone (food hopper + bottle tip + residual zone, Fig S12), total distance traveled (Fig S13), and velocity (Fig S14), did not show any significant difference between treatment groups. Thus, here we show that activation of the MC3R, but not inhibition, during the fasting period, can affect the subsequent behavior of mice during refeeding.

In summary, we have identified the expression of MC3R neurons in the thalamus, predominantly in the anterior to posterior axis of the PVT. Furthermore, we have uncovered that these neurons have a dynamic response to fasting dependent on the time of day of the fast, and that fasting-induced decreases in pCREB appear greater in female mice. We could demonstrate that MC3R modulation during the fasting
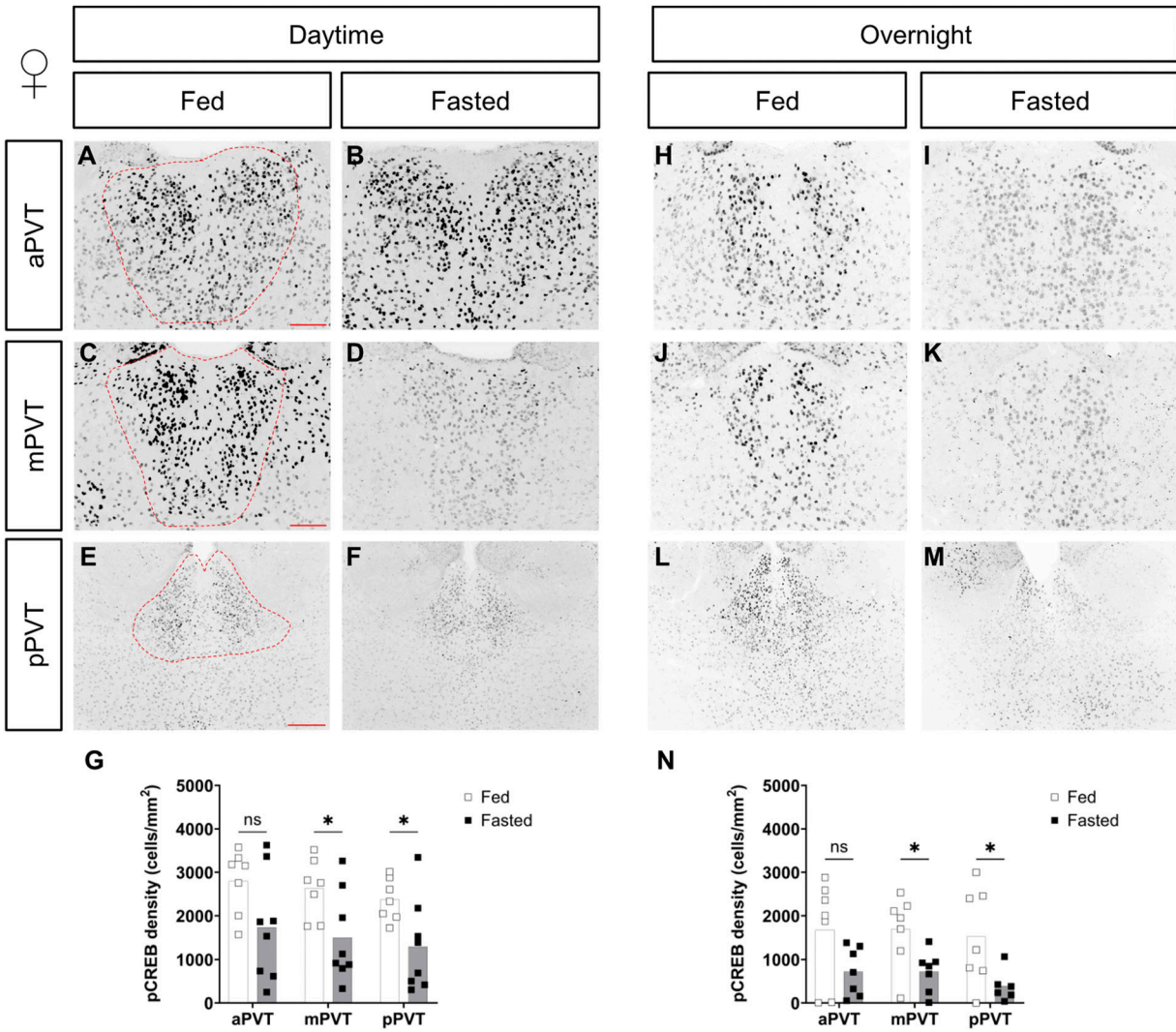
Figure 3. Comparison of pCREB cell density, in the paraventricular nucleus of the thalamus (PVT), of fed versus fasted female mice.
(A, B, C, D, E, F, G, H, I, J, K, L, M) Representative images of pCREB-positive cells in the anterior PVT (aPVT), mid PVT (mPVT), and posterior PVT (pPVT). **(A, C, E)** The red dashed outline in (A, C, E) represent regions of interest drawn around the PVT for analysis. **(G, N)** Quantification of pCREB cell density in daytime (G) and overnight (N) fasting experiments. **(E)** Scale bars in (A, C) are 100 and 200 μm in (E). Unpaired Welch t tests: *$P \leq 0.05$, ns, non-significant.
Source data are available for this figure.

period does not affect the amount of food eaten, during the refeeding period, nor the amount of body weight regain that occurs. However, we do show significant alterations in behavioral patterns in the immediate period after re-exposure to food. These results indicate that MC3R neuronal modulation may be necessary to fine tune the feeding behavioral response to result in a restoration of energy homeostasis.

Discussion

Here we indicate distinct neuroanatomical distributions of the MC3R throughout various thalamic nuclei. Specific focus on the PVT shows extensive expression of the MC3R throughout the anterior to posterior axis of this nucleus. Probing the interaction of the PVT with energy state changes induced by fasting resulted in significant

overall decreases in pCREB activation in the PVT, with a specific effect within the MC3R neurons in this region. This alteration in activity was not associated with changes to AgRP neuropeptide projection density in the PVT. However, we cannot rule out changes to the overall neuronal activity of these AgRP neuronal projections, as fasting is known to increase neuronal activity within the ARC and increase the activity of AgRP neurons. Furthermore, optogenetic stimulation of AgRP projections to the PVT is known to increase feeding (Betley et al, 2013; Grzelka et al, 2023).

Inhibition of AgRP neuronal projections to PVT neurons in calorically restricted mice prevents food-seeking behavior (Wang et al, 2021). However, the opposite scenario, chronic activation of the circuit in an ad libitum state, does not elicit or drive food-seeking behavior (Wang et al, 2021). This suggests that AgRP to PVT connectivity is more strongly associated with seeking food in an energy-deprived state. Interestingly, whereas we did not see any
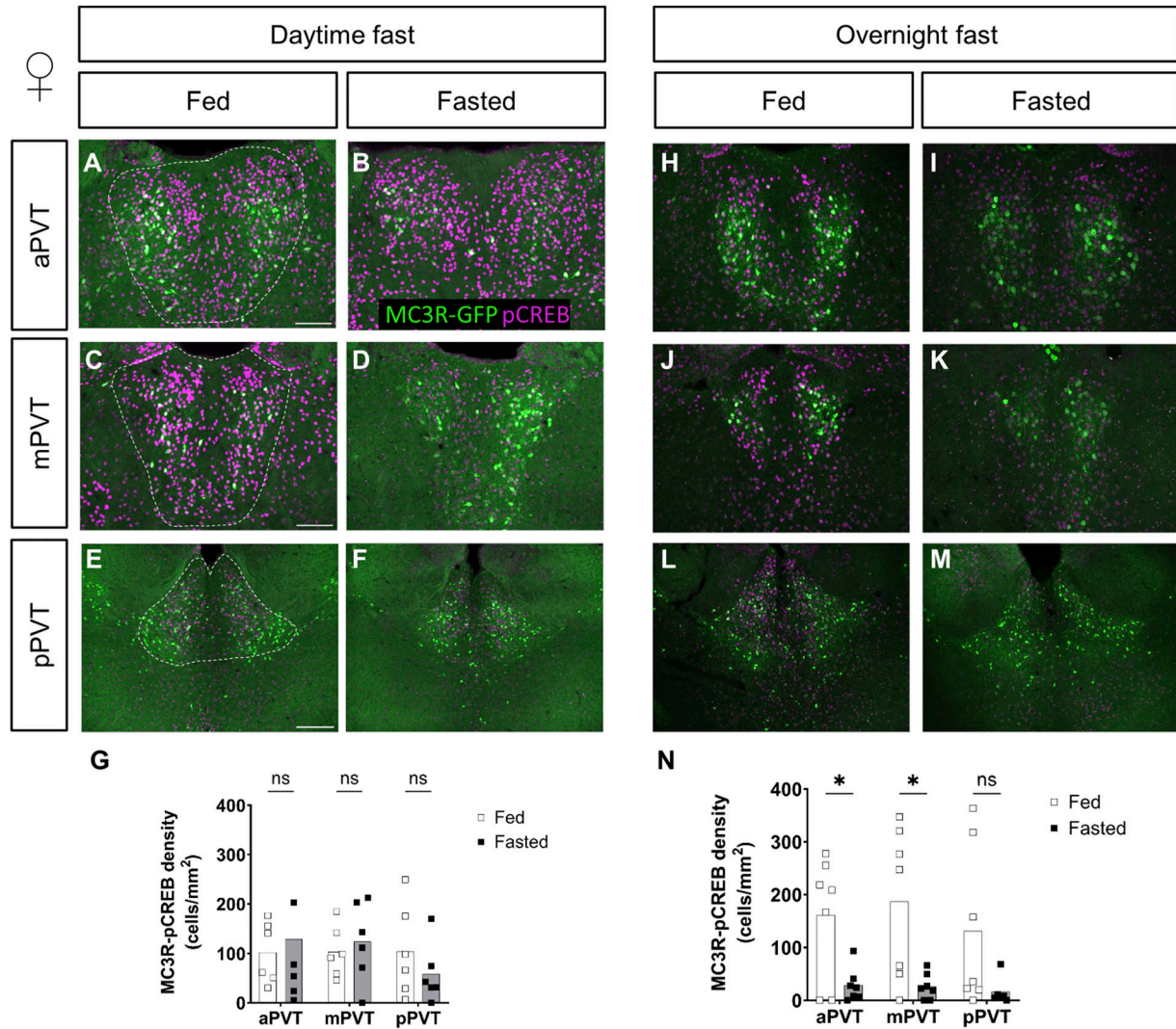
Figure 4. Comparison of MC3R-GFP/pCREB colocalized cell density, in the paraventricular nucleus of the thalamus (PVT), of fed versus fasted female mice.
(A, B, C, D, E, F, G, H, I, J, K, L, M) Representative images of MC3R-GFP– and pCREB-positive cells in the anterior PVT (aPVT), mid PVT (mPVT), and posterior PVT (pPVT). **(A, C, E)** The white dashed outline in (A, C, E) represent regions of interest drawn around the PVT for analysis. **(G, N)** Quantification of colocalized cell density in daytime (G) and overnight (N) fasting experiment. **(E)** Scale bars in (A, C) are 100 and 200 μm in (E). Unpaired Welch t tests: *$P \leq 0.05$, ns, non-significant.
Source data are available for this figure.

significant alteration of body weight change upon refeeding, indicative of the matched food intake between the groups, an analysis of the time spent in various regions of the cage and distance traveled within the refeeding period uncovered unique changes. Activation of MC3R neurons during fasting led to greater time being spent at the food hopper (and the tip of the water bottle) after the food was present. This increased interaction with the food hopper is interesting given the documented role of MC3R in food anticipatory activity. In normal animals, an increase in locomotor activity is noted before the presentation of food; however, MC3R-deficient animals show a significant defect in food anticipatory activity (Sutton et al, 2008, 2010). Our data would suggest that hyperactivation of MC3R in the fasting period results in potential increases in food anticipatory behavior, food arousal or food attention. However, the exact behavioral changes and their

underlying networks need further investigation. In our model, we cannot rule out that the chemogenetic modulation of neuronal activity is also affecting AgRP neurons, as up to 97% of AgRP neurons co-express the MC3R (Sweeney et al, 2021). Thus, when MC3R neurons, and by default many AgRP neurons of the ARC, are activated across the fasting period, this could potentially alter the neuronal response to food resulting in changes to feeding behavior. Indeed, one limitation of the model in our study is the expression of the DREADD receptors in all MC3R-positive cells throughout the body as driven by the MC3R-Cre model. However, as no difference in food intake itself was uncovered, it is likely that the MC3R effects are occurring outside the ARC. Subsequent studies will need to be performed to determine the possible contribution of peripheral MC3R activation and the specificity of PVT-MC3R cells in mediating this behavior.
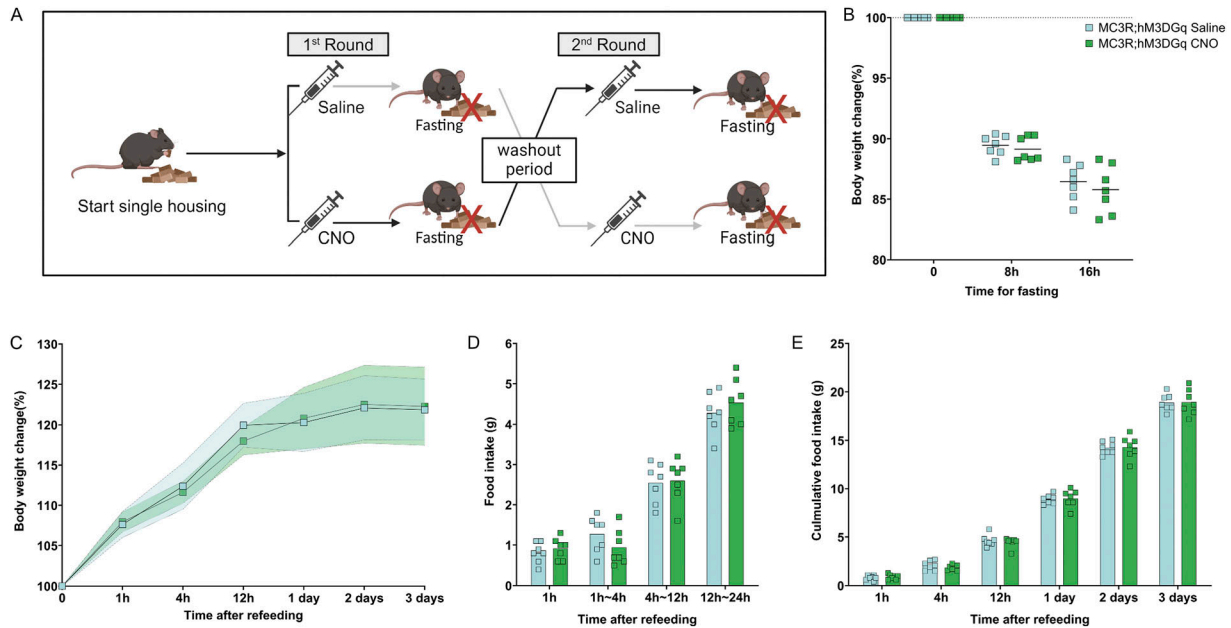
Figure 5. Activation of melanocortin 3 receptor (MC3R) neurons during overnight fasting in females.
(A, B) Experimental paradigm, (B) Body weight change during the fasting (in percentage) was plotted in comparison to the body weight at fasting, before the first injection. Body weight was measured at 8 h fasting before the second injection and 16 h before refeeding. **(C)** Body weight change after refeeding at different time points; data points indicate mean; colored area indicates SD. **(D)** Food intake was measured during refeeding at different time intervals. **(E)** Cumulative food intake (in grams) was measured during refeeding at different time points. **(B, C, D, E)** Blue indicates the MC3R; hM3DGq saline-treated control group and green indicates the MC3R; hM3DGq clozapine-*n*-oxide–treated group. N = 7 for both groups in all the graphs. Two-way ANOVA. No significance was detected.
Source data are available for this figure.

Recent heightened interest in the MC3R has proposed a functional role in driving sexually dimorphic anorectic behaviors. Specifically, probing PVT activity in response to refeeding after a fast shows dramatic increases in c-Fos expression across the anterior-to-posterior axis (Cho et al, 2023). Assessment of real-time activity of these neurons was probed in response to stressors in the environment and indeed the calcium-mediated activity was significantly altered in MC3R neurons. Here we show that, already in the fasting period, PVT neurons show decreased levels of pCREB in the mid and posterior PVT regions. Interestingly, this effect seems to be greater in female mice, which supports recent studies associating MC3R activity to anorexia-like phenotypes and increased effects on aspects such as novelty-suppressed feeding in female animals (Sweeney et al, 2021). In addition to this decrease in overall signal, there is also a significant overall decrease in pCREB labeling of the MC3R-positive neurons specifically. This was more dramatic in the overnight versus the daytime fasted groups, highlighting the likely importance of the recently described circadian rhythmicity of the AgRP neuronal activity in mediating aspects of this response (Sayar-Atasoy et al, 2024). In our study, the time of day of sample collection resulted in an apparent overall, and inverse, effect on c-Fos and pCREB labeling. This is consistent with known literature showing circadian rhythmicity of known hormones acting in this brain region, such as AgRP (Cedernaes et al, 2019; Sayar-Atasoy et al, 2024) or changes in glucocorticoids, whose circadian rhythm s also defective in MC3R KO animals (Renquist et al, 2012).

Whereas changes in markers of neuronal activity in MC3R neurons are noted and have sex-specific effects, the causative

mechanism for this potential sexual dimorphism remains elusive. In addition, the exact downstream effects of changes to MC3R neuronal activity are not known. As more studies delineate the ARC^AgRP to PVT^MC3R neuronal connections and their role in various PVT-mediated behaviors, it will be critical to understand the real-time activity changes and modulation of further MC3R neuronal targets to build upon our knowledge of neurocircuit activity fluxes and effects on feeding behaviors in various metabolic and environmental contexts.

These changes to behavior and the underlying neuronal circuits in this acute (minutes to hours) time period are critical to understanding and improving interventional strategies for curbing altered feeding behaviors. These small alterations in feeding, the acute changes to neurocircuit activity and connectivity, and the associated changes to the whole-body physiological responses may ultimately result in a combined contribution to long-term metabolic dysfunction and the gradual accumulation of body weight.

Materials and Methods

Mice

All mice were bred within the animal facility at the Max-Rubner Laboratory at the German Institute for Human Nutrition, Potsdam-Rehbrücke (DIfE). Mice were group housed in individually vented
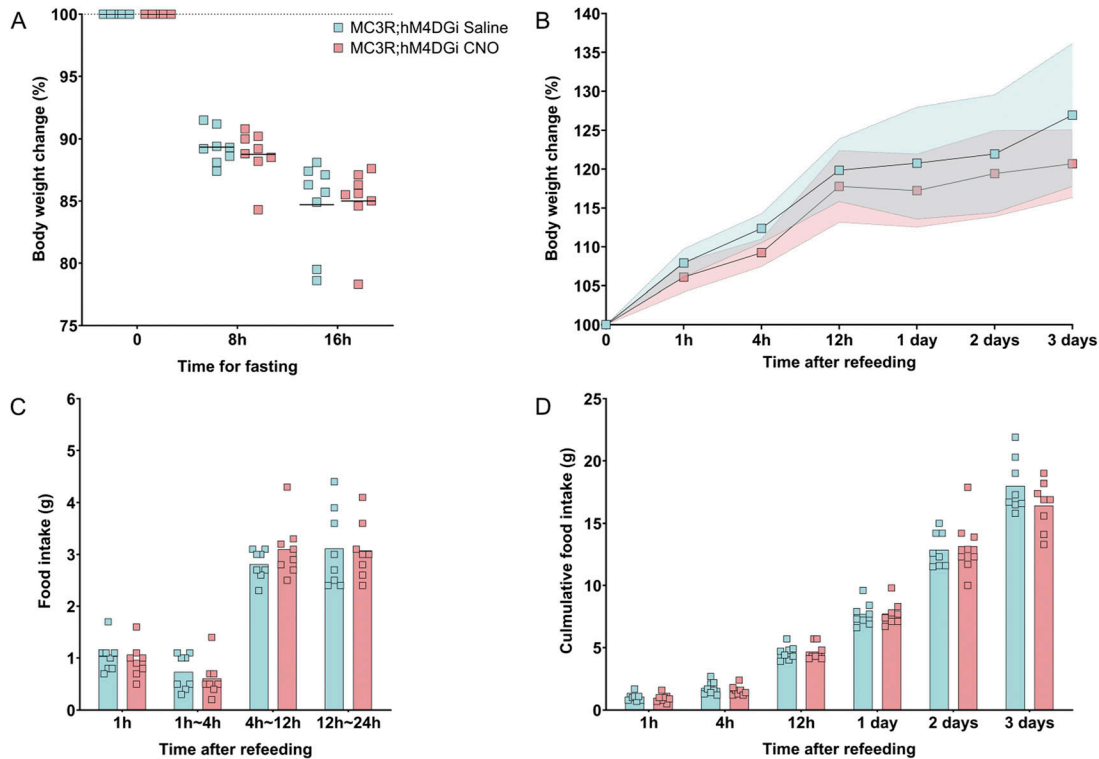
Figure 6.   Inhibition of melanocortin 3 receptor (MC3R) neurons during overnight fasting in females.
(A) Body weight change during fasting (in percentage) was plotted in comparison to the body weight at fasting, before the first injection. Body weight was measured at 8 h fasting before the second injection, and 16 h before refeeding. **(B)** Body weight change after refeeding at different time points, data points indicate mean, colored area indicates SD. **(C)** Food intake (in grams) was measured during refeeding at different time intervals. **(D)** Cumulative food intake (in grams) was measured during refeeding at different time points. **(A, B, C, D)** Blue indicates MC3R; hM4DGi saline-treated control group and pink indicates MC3R; hM4DGi clozapine-*n*-oxide–treated group. N = 8 for both groups in all the graphs. Two-way ANOVA. No significance was detected.
Source data are available for this figure.

cages (IVC) cages, with ad libitum access (unless otherwise stated) to food and sterile acidified water, under a 12-h on/off light cycle, and an RT of 22 ± 2°C. All experiments were approved by the Landesamt für Arbeitschutz, Verbraucherschutz, und Gesundheit (Land Brandenburg, Germany), under applications 2347-13-2021, 2347-42-2020, 2347-31-2021, and T-04-20-NDF, and conducted in compliance with the ARRIVE guidelines and the EU directive 2010/63/EU.

Transgenic MC3R-GFP (Tg [Mc3r-EGFP] BX153Gsat) (Gong et al, 2003; Heintz, 2004) mice were provided by Dr. Roger Cone and maintained on an FVB/N background. MC3R-Cre mice (Ghamari-Langroudi et al, 2018) were provided by Dr. Roger Cone and maintained on a C57BL6/N (>5 generations from C57BL6J) background. R26-LSL-RSR-hM4DGi-ZsGreen (De Solis et al, 2024) expressing mice that had previously bred to Deleter-Dre mice to remove the rox-flanked stop codon or R26-LSL-hM3DGq-eGFP (Steculorum et al, 2016) expressing animals were provided by Dr. Jens Brüning and were maintained on a C57BL6N background. When crossed with MC3R-Cre, this allows for the expression of the hM3DGq or hM4DGi in all MC3R-positive cells.

Genotyping of mice was carried out via PCR using the following primers and annealing temperatures listed in Table 1. The PCR cycling conditions were as follows: step 1: 95°C for 5 min; step 2:

95°C for 30 s; step 3: annealing (see Table 1); step 4: 72°C for 1 min (steps 2–4 repeated for 35 cycles); step 5: 72°C for 5 min. The resulting PCR products were separated on a 1% agarose gel.

Fed-fasting

In all fasting experiments, 2–3-mo-old mice, in both fed and fasted groups, were placed into a new cage and access to food was removed from the fasted group for 16–17 h. Overnight fasting began at "Lights OFF" (ZT12). Daytime fasting began 4 h after "Lights ON" (ZT4). In Figs 2, 3, 4, S1, S2, S3, S4, S5, S6, and S7, mice in both fed and fasted groups were euthanized at the end of the fasting period.

Fasting refeed

The fasting refeed experiment (in Figs 5 and 6) used 2–3-mo-old MC3R-Cre; ROSA26-LSL-hM3DGq-eGFP and MC3R-Cre; ROSA26-LSL-hM4DGi mice. For more accurate measurement of food and avoidance of fighting during fasting, animals were single housed. They were allowed to acclimate to single housing and human handling for 1 wk. Intraperitoneal (i.p.) injections of saline were given for 3 d before fasting to minimize the stress caused by injection. Upon fasting, the mice were weighed and then received i.p. injections of either CNO (MC3R-Cre; ROSA26-LSL-hM3DGq mice, 0.3
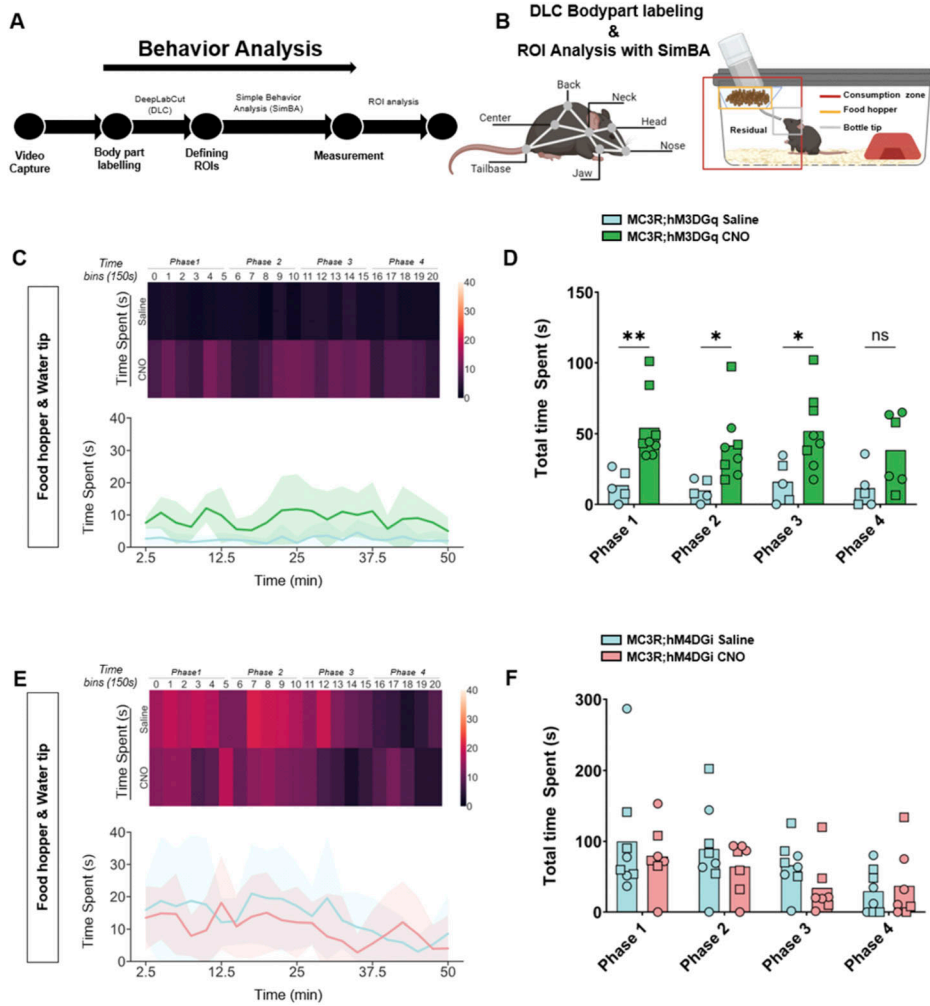
Figure 7. Behavior tracking during refeeding after melanocortin 3 receptor (MC3R) activation or inhibition.

(A) Analysis pipeline after video capture of animal behavior with refeeding. (B) Indications of body part labeling with DeepLabCut and analysis of regions of interest with SimBA. Selection of regions of interests within the home cage is indicated in the graphic. (C) Time spent at the food hopper (and bottle tip) in saline- and clozapine-*n*-oxide (CNO)–treated MC3R; hM3DGq mice visualized with a heat map ((C) top) or line graphs ((C) bottom). (D) Total time spent at the food hopper (and bottle tip) during time bins 0–5 (Phase 1), 6–10 (Phase 2), 11–15 (Phase 3), and 16–20 (Phase 4). Blue indicates the MC3R; hM3DGq saline-treated control group and green indicates the MC3R; hM3DGq CNO-treated group. Male data points are represented as circles and female data points as squares. (E) Time spent at the food hopper (and bottle tip) in saline- and CNO-treated MC3R; hM4DGi mice visualized with a heat map ((E) top) or line graphs ((E) bottom). (F) Total time spent at the food hopper (and bottle tip) during time bins 0–5 (Phase 1), 6–10 (Phase 2), 11–15 (Phase 3), and 16–20 (Phase 4). Blue indicates the MC3R; hM3DGq saline-treated control group and pink indicates the MC3R; hM4DGi CNO-treated group. Male data points are represented as circles and female data points as squares. (D) Two-way ANOVA (D, F), with Šídák's multiple comparisons test (D): *$P \le 0.05$, **$P \le 0.01$, ns, non-significant.
Source data are available for this figure.

Table 1. Genotyping primers and annealing temperatures.

	Target	Sequence (5'-3')	Product	Annealing temperature (time)
1	MC3R-Cre	Cre_WT (mom0137) CTGCAGTTCGATCACTGGAAC	WT: 542 bp	66°C (30 s)
		Cre_Common (mom0138) AAAGGCCTCTACAGTCTATAG		
		Cre_Mut1 (oIMR6694) TCCAATTTACTGACCGTACA	Tg: 450 bp	
		Cre_Mut2 (oIMR6695) TCCTGGCAGCGATCGCTATT		
2	MC3R-GFP	GFP116 Rev: ACA GCT CGT CCA TGC CGA GAG	WT: 325 bp	56°C (45 s)
		GFP115 Fwd: GAT GCC ACC TAC GGC AAG CTG		
		MC3R_GFP WT rev: GATGAAGACCTGCTCACAGAACCCAC	Tg: 600 bp	
		MC3R_GFP Fwd: AGGAAAGTTCTTTCTATGTCTCCAAGCCC		
3	hM3DGq and hM4DGI	Forward CAGGS: AAA GTC GCT CTG AGT TGT TAT C	WT: 570 bp	56°C (45 s)
		Rev-WT: GAT ATG AAG TAC TGG GCT CTT		
		Rev CAGGS: TGT CGC AAA TTA ACT GTG AAT C	Floxed: 380 bp	

mg/kg, 10 µl/g BW and for MC3R-Cre; ROSA26-LSL-hM4DGi 3 mg/, 10 µl/g BW) or saline (0.9%, 10 µl/g BW). The same solutions were then given again 8 h later, to ensure activation/inhibition of MC3R neurons throughout the fasting period. Mice were fasted overnight, from ZT 11 to ZT 3. At refeeding, the mice were video recorded. Their body weight change and food intake were measured at 1, 3, 6, 12, and

Table 2.   Primary antibodies used in immunohistochemistry experiments.

	Primary antibody	Host	Supplier	Catalog number	Dilution
1	Agouti-related peptide (AGRP)	Rabbit	Phoenix	H-003-53	1 in 40,000
2	c-Fos	Rat	Synaptic Systems	226 017	1 in 1,000
3	GFP	Rabbit	Invitrogen	A-6455	1 in 5,000
4	GFP	Chicken	Abcam	ab13970	1 in 5,000
5	Phospho-CREB (ser133)	Rabbit	Cell Signaling	#9198	1 in 2,000

Table 3.   Secondary antibodies used in immunohistochemistry experiments.

Secondary antibody	Supplier	Catalog number	Dilution	Used against primary antibody
Alexa Fluor 594 donkey anti-rabbit	Invitrogen	A21207	1 in 500	1 and 5
Alexa Fluor 633 donkey anti-rat	Sigma-Aldrich	SAB4600133	1 in 500	2
Alexa Fluor 488 donkey anti-rabbit	Invitrogen	A21206	1 in 500	3
Alexa Fluor 488 donkey anti-chicken	Dianova	703-545-155	1 in 1,000	4

24 h time points. To minimize animal numbers required for this experiment, a cross-over design was implemented: after a 2-wk wash-out period, the same mice underwent the same treatment procedure, but with the opposite treatment option (CNO or saline).

Euthanasia and tissue processing

At euthanasia, mice were transcardially perfused with PBS followed by 4% PFA in borate buffer (pH 9.5) (#441244; Sigma-Aldrich), under pentobarbital anaesthesia (400 mg/kg; i.p.) diluted in isotonic sodium chloride solution (#1021010; Delta-medica). Whole brains were harvested and post-fixed in 4% PFA for 4–24 h, at 4°C. Brains were then dehydrated in 20% sucrose in PBS, overnight at 4°C, before being frozen at –80°C for further processing.

Frozen brains were then sliced into 30µm-thick coronal sections using a sliding microtome (#400410, Slide 4004 M; pfm medical) and serial sections were stored in glycerol-containing PBS solution at –20°C, until further use.

Immunohistochemistry

Coronal brain sections including the PVT were first treated in 0.3% glycine for 10 min, followed by permeabilization for 10 min in 0.03% SDS. Next sections were blocked in 3% normal donkey serum in 0.125% Triton-X in K-PBS for 1 h at RT. Slices were then immunostained with primary antibodies in SignalStain solution (#8112; Cell Signaling) at 4°C overnight, as detailed in Table 2. Next, sections were washed in K-PBS 3 times for 10 min before being labeled with secondary antibodies, as detailed in Table 3. Finally, stained sections were mounted on Superfrost glass slides (J800AMNZ; Epredia) and coverslipped with VECTASHIELD Antifade Mounting Medium containing DAPI (#VEC-H-1200; Biozol).

Image acquisition and analysis

Multi-channel Z-stack images of representative sections of the anterior PVT (from bregma –0.71 to –0.95 mm), mid PVT (from bregma –1.23 to –1.43 mm), and posterior PVT (from bregma –1.67 to –1.79 mm) were acquired at 20× magnification, using either a Zeiss Confocal Microscope (GFP-c-Fos and GFP-AgRP images) or a Zeiss Fluorescent Axio Observer Microscope equipped with Apotome 3 (GFP-pCREB images). One image per PVT region was acquired. Image processing and analysis were performed using custom-written macros in ImageJ software v2.1.0 (National Institute of Health).

For all image analysis, multi-channel z-stack images were compressed into a single plane in the z-axis using the maximum intensity projection function and split into separate channels. A region of interest (ROI) was manually drawn around the limits of the PVT using the GFP channel from each image and applied to the channel to be analyzed (GFP/c-Fos/pCREB/AgRP).

For cell density measurements, a threshold was automatically determined for the channel to be analyzed and converted to a binary image. In the GFP-c-Fos staining, the c-Fos channel was thresholded using the *Triangle* algorithm, and the GFP channel using the *Moments* algorithm. In the GFP-pCREB staining, a threshold for both channels was determined using *Triangle*. Images were then *despeckled* to remove noise and *watershed* to define individual cells. The *Analyze particles* plugin was then used, with the following minimum cell size, to automatically count the number of positive immunolabeled cells in the ROI: c-Fos and pCREB = 20 μm^2, GFP and colocalized cells = 40 μm^2. The number of cells was then divided by the ROI area to yield cell density measurements.

For fiber density measurements, the AgRP channel was automatically thresholded using the *Triangle* algorithm in ImageJ and converted to a binary image. The raw integrated density value (representing the total number of pixels containing positive immunolabeling) was measured and divided by the total area of the

ROI analyzed, yielding the percentage area of positive immuno-labeling (fiber density).

For both cell density and fiber density measurements, thresh-olded binary images were compared with the original images as a quality check. Images whereby the thresholding did not accurately detect cells/axon fibers were excluded from further analysis.

DeepLabCut model and SimBA ROI analysis of refeeding behavior

During the refeeding experiment, Anymaze software (Stoelting) was used to generate video recordings of mice in regular IVC cages after a 16-h fast. Two machine-learning toolkits for animal behavior analysis were used, DeepLabCut (DLC) (Mathis et al, 2018) and Simple Behavior Analysis (SimBA) (Popik et al, 2023). These software programs were downloaded from (https://github.com/DeepLabCut) and (https://github.com/sgoldenlab/simba), respectively, and installed on a workstation with the following specifications: AMD Ryzon 9 7900X 12-Core Processor, with a speed of 4.70 GHz and RAM of 64.0 GB in Windows 10. Using the DLC version 2.3.5, a 7-body part labeling system was implemented, namely the nose, head, jaw, neck, back, center, and tail base (see Fig 7B). An experimenter blinded to the experiment manually labeled a total of 300 randomly sampled frames from 10 videos. The labeled frames were then used to train a machine model of 700,000 epochs or iterations with a p_{cutoff} of 0.6. Validation of the trained network yielded the following results for 700,000 iterations: a training error of 1.12 pixels and a test error of 2.7 pixels. The trained model was then validated on a separate set of videos and finally used to analyze all video recordings. The subsequent DLC pose estimation coordinates of all labeled body parts were then transferred into SimBA. In SimBA, a novel 7-node-body configuration was generated based on the captured videos, which were side views, for classical tracking of mice. Using this side-view tracking format, the DeepPoseKit CSV files were imported from DLC, and the following SimBA modifications were carried out. First, the imported CSV files were interpolated using the quadratic interpolation method together with Gaussian smoothing of 200 ms. Afterward, a distance of 195 mm was used to calibrate the pixels to the distance for each video, which is the height of the IVC cages used in the experiments. Furthermore, an outlier correction with 1.0 criteria was performed for both location and movement, respectively, together with the mean aggregation method. This step was critical to excluding all non-specific labeling. Then, 3 ROIs were drawn, namely, the water, food, and consumption zones, as shown in Fig 7B. The distance traveled (m) and velocity (cm/s) of each mouse were measured using the ROI Data Aggregates and time bins analysis functions in SimBA. The time spent within each of the ROIs was quantified using the probability threshold of 0.25, to account for instances where the mouse enters the provided housing structure and thus may be absent from the frame. The analysis of the videos was split into time bins of 150 s for a total of 20-time bins corresponding to 50 min of behavior video capture. The read-outs from SimBA were further processed using Python (3.11.4) to measure time spent, distance traveled, and velocity: The time spent by each mouse in the residual zone was estimated by subtracting the time spent at both the food hopper and bottle tip from the time spent at the consumption zone.

Statistical analysis

Bar graphs show all individual data points and group means. All graphs and inferential statistics were created using GraphPad Prism 10.1.2 (GraphPad Software) or performed in Python. Unpaired two-tailed Welch's t tests were performed to analyze cell density and fiber density differences between groups. For behavioral tracking data across time, a two-way ANOVA was performed to determine overall main effects, and followed up (where necessary) with Šídák's multiple comparisons test. Statistical significance was set at an alpha value of 0.05. All data pertaining to specific statistical tests, n-numbers and significance can be found summarized in Table S1.

Supplementary Information

Supplementary Information is available at https://doi.org/10.26508/lsa.202402754.

Acknowledgements

Author Contributions

RA Chesters: conceptualization, data curation, software, formal analysis, supervision, validation, investigation, visualization, methodology, project administration, and writing—original draft, review, and editing.

J Zhu: conceptualization, data curation, formal analysis, supervision, validation, investigation, visualization, methodology, project administration, and writing—original draft, review, and editing.

BM Coull: conceptualization, data curation, software, formal analysis, supervision, validation, investigation, methodology, project administration, and writing—review and editing.

D Baidoe-Ansah: data curation, software, formal analysis, supervision, validation, visualization, methodology, and writing—review and editing.

L Baumer: data curation, formal analysis, investigation, and writing—review and editing.

L Palm: data curation, formal analysis, investigation, and writing—review and editing.

N Klinghammer: data curation, formal analysis, and writing—review and editing.

S Chen: investigation and writing—review and editing.

A Hahm: investigation and writing—review and editing.

S Yagoub: investigation and writing—review and editing.

L Cantacorps: investigation and writing—review and editing.

D Bernardi: investigation and writing—review and editing.

K Ritter: investigation and writing—review and editing.

RN Lippert: conceptualization, data curation, formal analysis, supervision, funding acquisition, validation, investigation, visualization, methodology, project administration, and writing—original draft, review, and editing.

Conflict of Interest Statement

The authors declare that they have no conflict of interest.

References

Alexander GM, Rogan SC, Abbas AI, Armbruster BN, Pei Y, Allen JA, Nonneman RJ, Hartmann J, Moy SS, Nicolelis MA, et al (2009) Remote control of neuronal activity in transgenic mice expressing evolved G protein-coupled receptors. *Neuron* 63: 27–39. doi:10.1016/j.neuron.2009.06.014

Alhadeff AL, Goldstein N, Park O, Klima ML, Vargas A, Betley JN (2019) Natural and drug rewards engage distinct pathways that converge on coordinated hypothalamic and reward circuits. *Neuron* 103: 891–908.e6. doi:10.1016/j.neuron.2019.05.050

Anisimova M, Lamothe-Molina PJ, Franzelin A, Aberra AS, Hoppa MB, Gee CE, Oertner TG (2023) Neuronal FOS reports synchronized activity of presynaptic neurons. *BioRxiv*. doi:10.1101/2023.09.04.556168 (Preprint posted September 05, 2023).

Aris IM, Tint MT, Teh AL, Holbrook JD, Quah PL, Chong MF, Lin X, Soh SE, Saw SM, Kwek K, et al (2016) MC3R gene polymorphisms are associated with early childhood adiposity gain and infant appetite in an Asian population. *Pediatr Obes* 11: 450–458. doi:10.1111/ijpo.12086

Atasoy D, Betley JN, Su HH, Sternson SM (2012) Deconstruction of a neural circuit for hunger. *Nature* 488: 172–177. doi:10.1038/nature11270

Bartel DP, Sheng M, Lau LF, Greenberg ME (1989) Growth factors and membrane depolarization activate distinct programs of early response gene expression: Dissociation of fos and jun induction. *Genes Dev* 3: 304–313. doi:10.1101/gad.3.3.304

Bedenbaugh MN, Brener SC, Maldonado J, Lippert RN, Sweeney P, Cone RD, Simerly RB (2022) Organization of neural systems expressing melanocortin-3 receptors in the mouse brain: Evidence for sexual dimorphism. *J Comp Neurol* 530: 2835–2851. doi:10.1002/cne.25379

Begriche K, Marston OJ, Rossi J, Burke LK, McDonald P, Heisler LK, Butler AA (2012) Melanocortin-3 receptors are involved in adaptation to restricted feeding. *Genes Brain Behav* 11: 291–302. doi:10.1111/j.1601-183X.2012.00766.x

Betley JN, Cao ZF, Ritola KD, Sternson SM (2013) Parallel, redundant circuit organization for homeostatic control of feeding behavior. *Cell* 155: 1337–1350. doi:10.1016/j.cell.2013.11.002

Biglari N, Gaziano I, Schumacher J, Radermacher J, Paeger L, Klemm P, Chen W, Corneliussen S, Wunderlich CM, Sue M, et al (2021) Functionally distinct POMC-expressing neuron subpopulations in hypothalamus revealed by intersectional targeting. *Nat Neurosci* 24: 913–929. doi:10.1038/s41593-021-00854-0

Brandt C, Nolte H, Henschke S, Engstrom Ruud L, Awazawa M, Morgan DA, Gabel P, Sprenger HG, Hess ME, Günther S, et al (2018) Food perception primes hepatic ER homeostasis via melanocortin-dependent control of mTOR activation. *Cell* 175: 1321–1335.e20. doi:10.1016/j.cell.2018.10.015

Bruning JC, Fenselau H (2023) Integrative neurocircuits that control metabolism and food intake. *Science* 381: eabl7398. doi:10.1126/science.abl7398

Butler AA, Kesterson RA, Khong K, Cullen MJ, Pelleymounter MA, Dekoning J, Baetscher M, Cone RD (2000) A unique metabolic syndrome causes obesity in the melanocortin-3 receptor-deficient mouse. *Endocrinology* 141: 3518–3521. doi:10.1210/endo.141.9.7791

Butler AA, Girardet C, Mavrikaki M, Trevaskis JL, Macarthur H, Marks DL, Farr SA (2017) A life without hunger: The ups (and downs) to modulating melanocortin-3 receptor signaling. *Front Neurosci* 11: 128. doi:10.3389/fnins.2017.00128

Cedernaes J, Huang W, Ramsey KM, Waldeck N, Cheng L, Marcheva B, Omura C, Kobayashi Y, Peek CB, Levine DC, et al (2019) Transcriptional basis for rhythmic control of hunger and metabolism within the AgRP neuron. *Cell Metab* 29: 1078–1091.e5. doi:10.1016/j.cmet.2019.01.023

Chen Y, Knight ZA (2016) Making sense of the sensory regulation of hunger neurons. *Bioessays* 38: 316–324. doi:10.1002/bies.201500167

Chen Y, Lin YC, Kuo TW, Knight ZA (2015) Sensory detection of food rapidly modulates arcuate feeding circuits. *Cell* 160: 829–841. doi:10.1016/j.cell.2015.01.033

Chen W, Mehlkop O, Scharn A, Nolte H, Klemm P, Henschke S, Steuernagel L, Sotelo-Hitschfeld T, Kaya E, Wunderlich CM, et al (2023) Nutrient-sensing AgRP neurons relay control of liver autophagy during energy deprivation. *Cell Metab* 35: 786–806.e13. doi:10.1016/j.cmet.2023.03.019

Cheng J, Wang J, Ma X, Ullah R, Shen Y, Zhou YD (2018) Anterior paraventricular thalamus to nucleus accumbens projection is involved in feeding behavior in a novel environment. *Front Mol Neurosci* 11: 202. doi:10.3389/fnmol.2018.00202

Cho D, O'Berry K, Possa-Paranhos IC, Butts J, Palanikumar N, Sweeney P (2023) Paraventricular thalamic MC3R circuits link energy homeostasis with anxiety-related behavior. *J Neurosci* 43: 6280–6296. doi:10.1523/JNEUROSCI.0704-23.2023

Clark AM, Leroy F, Martyniuk KM, Feng W, McManus E, Bailey MR, Javitch JA, Balsam PD, Kellendonk C (2017) Dopamine D2 receptors in the paraventricular thalamus attenuate cocaine locomotor sensitization. *eNeuro* 4: ENEURO.0227-17.2017. doi:10.1523/ENEURO.0227-17.2017

Cone RD (1999) The central melanocortin system and energy homeostasis. *Trends Endocrinol Metab* 10: 211–216. doi:10.1016/s1043-2760(99)00153-8

Cone RD (2005) Anatomy and regulation of the central melanocortin system. *Nat Neurosci* 8: 571–578. doi:10.1038/nn1455

de Moura E Dias M, Dos Reis SA, da Conceição LL, Sediyama CmNdO, Pereira SS, de Oliveira LL, Gouveia Peluzio MdC, Martinez JA, Milagro FI (2021) Diet-induced obesity in animal models: Points to consider and influence on metabolic markers. *Diabetol Metab Syndr* 13: 32. doi:10.1186/s13098-021-00647-2

De Solis AJ, Del Rio-Martin A, Radermacher J, Chen W, Steuernagel L, Bauder CA, Eggersmann FR, Morgan DA, Cremer AL, Sué M, et al (2024) Reciprocal activity of AgRP and POMC neurons governs coordinated control of feeding and metabolism. *Nat Metab* 6: 473–493. doi:10.1038/s42255-024-00987-z

Dietrich MO, Horvath TL (2013) Hypothalamic control of energy balance: Insights into the role of synaptic plasticity. *Trends Neurosci* 36: 65–73. doi:10.1016/j.tins.2012.12.005

Do-Monte FH, Minier-Toribio A, Quinones-Laracuente K, Medina-Colon EM, Quirk GJ (2017) Thalamic regulation of sucrose seeking during unexpected reward omission. *Neuron* 94: 388–400.e4. doi:10.1016/j.neuron.2017.03.036

Dong X, Li S, Kirouac GJ (2020) A projection from the paraventricular nucleus of the thalamus to the shell of the nucleus accumbens contributes to footshock stress-induced social avoidance. *Neurobiol Stress* 13: 100266. doi:10.1016/j.ynstr.2020.100266

Ellacott KL, Cone RD (2004) The central melanocortin system and the integration of short- and long-term regulators of energy homeostasis. *Recent Prog Horm Res* 59: 395–408. doi:10.1210/rp.59.1.395

Gao C, Leng Y, Ma J, Rooke V, Rodriguez-Gonzalez S, Ramakrishnan C, Deisseroth K, Penzo MA (2020) Two genetically, anatomically and functionally distinct cell types segregate across anteroposterior axis of paraventricular thalamus. *Nat Neurosci* 23: 217–228. doi:10.1038/s41593-019-0572-3

Ghamari-Langroudi M, Cakir I, Lippert RN, Sweeney P, Litt MJ, Ellacott KLJ, Cone RD (2018) Regulation of energy rheostasis by the melanocortin-3 receptor. *Sci Adv* 4: eaat0866. doi:10.1126/sciadv.aat0866

Ginty DD, Bading H, Greenberg ME (1992) Trans-synaptic regulation of gene expression. *Curr Opin Neurobiol* 2: 312–316. doi:10.1016/0959-4388(92)90121-z

Girardet C, Mavrikaki MM, Stevens JR, Miller CA, Marks DL, Butler AA (2017) Melanocortin-3 receptors expressed in Nkx2.1(+ve) neurons are sufficient for controlling appetitive responses to hypocaloric conditioning. *Sci Rep* 7: 44444. doi:10.1038/srep44444

Gong S, Zheng C, Doughty ML, Losos K, Didkovsky N, Schambra UB, Nowak NJ, Joyner A, Leblanc G, Hatten ME, et al (2003) A gene expression atlas of the central nervous system based on bacterial artificial chromosomes. *Nature* 425: 917–925. doi:10.1038/nature02033

Grzelka K, Wilhelms H, Dodt S, Dreisow ML, Madara JC, Walker SJ, Wu C, Wang D, Lowell BB, Fenselau H (2023) A synaptic amplifier of hunger for regaining body weight in the hypothalamus. *Cell Metab* 35: 770–785.e5. doi:10.1016/j.cmet.2023.03.002

Gui Y, Dahir NS, Wu Y, Downing G, Sweeney P, Cone RD (2023) Melanocortin-3 receptor expression in AgRP neurons is required for normal activation of the neurons in response to energy deficiency. *Cell Rep* 42: 113188. doi:10.1016/j.celrep.2023.113188

Heintz N (2004) Gene expression nervous system atlas (GENSAT). *Nat Neurosci* 7: 483. doi:10.1038/nn0504-483

Horio N, Liberles SD (2021) Hunger enhances food-odour attraction through a neuropeptide Y spotlight. *Nature* 592: 262–266. doi:10.1038/s41586-021-03299-4

Iglesias AG, Flagel SB (2021) The paraventricular thalamus as a critical node of motivated behavior via the hypothalamic-thalamic-striatal circuit. *Front Integr Neurosci* 15: 706713. doi:10.3389/fnint.2021.706713

Ji RR, Rupp F (1997) Phosphorylation of transcription factor CREB in rat spinal cord after formalin-induced hyperalgesia: Relationship to c-fos induction. *J Neurosci* 17: 1776–1785. doi:10.1523/JNEUROSCI.17-05-01776.1997

Kato TM, Fujimori-Tonou N, Mizukami H, Ozawa K, Fujisawa S, Kato T (2019) Presynaptic dysregulation of the paraventricular thalamic nucleus causes depression-like behavior. *Sci Rep* 9: 16506. doi:10.1038/s41598-019-52984-y

Kinouchi K, Magnan C, Ceglia N, Liu Y, Cervantes M, Pastore N, Huynh T, Ballabio A, Baldi P, Masri S, et al (2018) Fasting imparts a switch to alternative daily pathways in liver and muscle. *Cell Rep* 25: 3299–3314.e6. doi:10.1016/j.celrep.2018.11.077

Kirouac GJ (2015) Placing the paraventricular nucleus of the thalamus within the brain circuits that control behavior. *Neurosci Biobehav Rev* 56: 315–329. doi:10.1016/j.neubiorev.2015.08.005

Kong D, Dagon Y, Campbell JN, Guo Y, Yang Z, Yi X, Aryal P, Wellenstein K, Kahn BB, Sabatini BL, et al (2016) A postsynaptic AMPK→p21-activated kinase pathway drives fasting-induced synaptic plasticity in AgRP neurons. *Neuron* 91: 25–33. doi:10.1016/j.neuron.2016.05.025

Li Y, Dong X, Li S, Kirouac GJ (2014) Lesions of the posterior paraventricular nucleus of the thalamus attenuate fear expression. *Front Behav Neurosci* 8: 94. doi:10.3389/fnbeh.2014.00094

Li C, Navarrete J, Liang-Guallpa J, Lu C, Funderburk SC, Chang RB, Liberles SD, Olson DP, Krashes MJ (2019) Defined paraventricular hypothalamic populations exhibit differential responses to food contingent on caloric state. *Cell Metab* 29: 681–694.e5. doi:10.1016/j.cmet.2018.10.016

Lippert RN, Ellacott KL, Cone RD (2014) Gender-specific roles for the melanocortin-3 receptor in the regulation of the mesolimbic dopamine system in mice. *Endocrinology* 155: 1718–1727. doi:10.1210/en.2013-2049

Lutz TA, Woods SC (2012) Overview of animal models of obesity. *Curr Protoc Pharmacol* Chapter 5: Unit5.61. doi:10.1002/0471141755.ph0561s58

Mathis A, Mamidanna P, Cury KM, Abe T, Murthy VN, Mathis MW, Bethge M (2018) DeepLabCut: Markerless pose estimation of user-defined body parts with deep learning. *Nat Neurosci* 21: 1281–1289. doi:10.1038/s41593-018-0209-y

Mazzone CM, Liang-Guallpa J, Li C, Wolcott NS, Boone MH, Southern M, Kobzar NP, Salgado IdA, Reddy DM, Sun F, et al (2020) High-fat food biases hypothalamic and mesolimbic expression of consummatory drives. *Nat Neurosci* 23: 1253–1266. doi:10.1038/s41593-020-0684-9

Meffre J, Sicre M, Diarra M, Marchessaux F, Paleressompoulle D, Ambroggi F (2019) Orexin in the posterior paraventricular thalamus mediates hunger-related signals in the nucleus accumbens core. *Curr Biol* 29: 3298–3306.e4. doi:10.1016/j.cub.2019.07.069

Millan EZ, Ong Z, McNally GP (2017) Paraventricular thalamus: Gateway to feeding, appetitive motivation, and drug addiction. *Prog Brain Res* 235: 113–137. doi:10.1016/bs.pbr.2017.07.006

Moro C, Magnan C (2021) GTTs and ITTs: Aim for shorter fasting times. *Nat Metab* 3: 1133. doi:10.1038/s42255-021-00455-y

Obregon AM, Amador P, Valladares M, Weisstaub G, Burrows R, Santos JL (2010) Melanocortin-3 receptor gene variants: Association with childhood obesity and eating behavior in Chilean families. *Nutrition* 26: 760–765. doi:10.1016/j.nut.2009.07.005

Otis JM, Zhu M, Namboodiri VMK, Cook CA, Kosyk O, Matan AM, Ying R, Hashikawa Y, Hashikawa K, Trujillo-Pisanty I, et al (2019) Paraventricular thalamus projection neurons integrate cortical and hypothalamic signals for Cue-reward processing. *Neuron* 103: 423–431.e4. doi:10.1016/j.neuron.2019.05.018

Pandit R, van der Zwaal EM, Luijendijk MCM, Brans MAD, van Rozen AJ, Oude Ophuis RJA, Vanderschuren LJMJ, Adan RAH, la Fleur SE (2015) Central melanocortins regulate the motivation for sucrose reward. *PLoS One* 10: e0121768. doi:10.1371/journal.pone.0121768

Pandit R, Omrani A, Luijendijk MC, de Vrind VAJ, Van Rozen AJ, Ophuis RJAO, Garner K, Kallo I, Ghanem A, Liposits Z, et al (2016) Melanocortin 3 receptor signaling in midbrain dopamine neurons increases the motivation for food reward. *Neuropsychopharmacology* 41: 2241–2251. doi:10.1038/npp.2016.19

Parsons MP, Li S, Kirouac GJ (2007) Functional and anatomical connection between the paraventricular nucleus of the thalamus and dopamine fibers of the nucleus accumbens. *J Comp Neurol* 500: 1050–1063. doi:10.1002/cne.21224

Pei H, Patterson CM, Sutton AK, Burnett KH, Myers MG, Jr., Olson DP (2019) Lateral hypothalamic Mc3R-expressing neurons modulate locomotor activity, energy expenditure, and adiposity in male mice. *Endocrinology* 160: 343–358. doi:10.1210/en.2018-00747

Penzo MA, Robert V, Tucciarone J, De Bundel D, Wang M, Van Aelst L, Darvas M, Parada LF, Palmiter RD, He M, et al (2015) The paraventricular thalamus controls a central amygdala fear circuit. *Nature* 519: 455–459. doi:10.1038/nature13978

Petrovich GD (2021) The function of paraventricular thalamic circuitry in adaptive control of feeding behavior. *Front Behav Neurosci* 15: 671096. doi:10.3389/fnbeh.2021.671096

Popik P, Cyrano E, Piotrowska D, Holuj M, Golebiowska J, Malikowska-Racia N, Potasiewicz A, Nikiforuk A (2023) Effects of ketamine on rat social behavior as analyzed by DeepLabCut and SimBA deep learning algorithms. *Front Pharmacol* 14: 1329424. doi:10.3389/fphar.2023.1329424

Renquist BJ, Murphy JG, Larson EA, Olsen D, Klein RF, Ellacott KL, Cone RD (2012) Melanocortin-3 receptor regulates the normal fasting response. *Proc Natl Acad Sci U S A* 109: E1489–E1498. doi:10.1073/pnas.1201994109

Roseberry AG, Stuhrman K, Dunigan AI (2015) Regulation of the mesocorticolimbic and mesostriatal dopamine systems by α-melanocyte stimulating hormone and agouti-related protein. *Neurosci Biobehav Rev* 56: 15–25. doi:10.1016/j.neubiorev.2015.06.020

Roselli-Rehfuss L, Mountjoy KG, Robbins LS, Mortrud MT, Low MJ, Tatro JB, Entwistle ML, Simerly RB, Cone RD (1993) Identification of a receptor for gamma melanotropin and other proopiomelanocortin peptides in the hypothalamus and limbic system. *Proc Natl Acad Sci U S A* 90: 8856–8860. doi:10.1073/pnas.90.19.8856

Rowson SA, Pleil KE (2021) Influences of stress and sex on the paraventricular thalamus: Implications for motivated behavior. *Front Behav Neurosci* 15: 636203. doi:10.3389/fnbeh.2021.636203

Sayar-Atasoy N, Aklan I, Yavuz Y, Laule C, Kim H, Rysted J, Alp MI, Davis D, Yilmaz B, Atasoy D (2024) AgRP neurons encode circadian feeding time. *Nat Neurosci* 27: 102–115. doi:10.1038/s41593-023-01482-6

Schwartz MW, Seeley RJ, Zeltser LM, Drewnowski A, Ravussin E, Redman LM, Leibel RL (2017) Obesity pathogenesis: An endocrine society scientific statement. *Endocr Rev* 38: 267–296. doi:10.1210/er.2017-00111

Sheng M, Greenberg ME (1990) The regulation and function of c-fos and other immediate early genes in the nervous system. *Neuron* 4: 477–485. doi:10.1016/0896-6273(90)90106-p

Steculorum SM, Ruud J, Karakasilioti I, Backes H, Engstrom Ruud L, Timper K, Hess ME, Tsaousidou E, Mauer J, Vogt MC, et al (2016) AgRP neurons control systemic insulin sensitivity via myostatin expression in Brown adipose tissue. *Cell* 165: 125–138. doi:10.1016/j.cell.2016.02.044

Suleiman JB, Mohamed M, Bakar ABA (2020) A systematic review on different models of inducing obesity in animals: Advantages and limitations. *J Adv Vet Anim Res* 7: 103–114. doi:10.5455/javar.2020.g399

Sutton GM, Perez-Tilve D, Nogueiras R, Fang J, Kim JK, Cone RD, Gimble JM, Tschöp MH, Butler AA (2008) The melanocortin-3 receptor is required for entrainment to meal intake. *J Neurosci* 28: 12946–12955. doi:10.1523/JNEUROSCI.3615-08.2008

Sutton GM, Begriche K, Kumar KG, Gimble JM, Perez-Tilve D, Nogueiras R, McMillan RP, Hulver MW, Tschöp MH, Butler AA (2010) Central nervous system melanocortin-3 receptors are required for synchronizing metabolism during entrainment to restricted feeding during the light cycle. *FASEB J* 24: 862–872. doi:10.1096/fj.09-142000

Sweeney P, Bedenbaugh MN, Maldonado J, Pan P, Fowler K, Williams SY, Gimenez LE, Ghamari-Langroudi M, Downing G, Gui Y, et al (2021) The melanocortin-3 receptor is a pharmacological target for the regulation of anorexia. *Sci Transl Med* 13: eabd6434. doi:10.1126/scitranslmed.abd6434

Wang C, Zhou W, He Y, Yang T, Xu P, Yang Y, Cai X, Wang J, Liu H, Yu M, et al (2021) AgRP neurons trigger long-term potentiation and facilitate food seeking. *Transl Psychiatry* 11: 11. doi:10.1038/s41398-020-01161-1

Wei W, Pham K, Gammons JW, Sutherland D, Liu Y, Smith A, Kaczorowski CC, O'Connell KMS (2015) Diet composition, not calorie intake, rapidly alters intrinsic excitability of hypothalamic AgRP/NPY neurons in mice. *Sci Rep* 5: 16810. doi:10.1038/srep16810

Wess J, Nakajima K, Jain S (2013) Novel designer receptors to probe GPCR signaling and physiology. *Trends Pharmacol Sci* 34: 385–392. doi:10.1016/j.tips.2013.04.006

West KS, Lu C, Olson DP, Roseberry AG (2019) Alpha-melanocyte stimulating hormone increases the activity of melanocortin-3 receptor-expressing neurons in the ventral tegmental area. *J Physiol* 597: 3217–3232. doi:10.1113/JP277193

Wu GY, Deisseroth K, Tsien RW (2001) Activity-dependent CREB phosphorylation: Convergence of a fast, sensitive calmodulin kinase pathway and a slow, less sensitive mitogen-activated protein kinase pathway. *Proc Natl Acad Sci U S A* 98: 2808–2813. doi:10.1073/pnas.051634198

Wu Q, Lemus MB, Stark R, Bayliss JA, Reichenbach A, Lockie SH, Andrews ZB (2014) The temporal pattern of cfos activation in hypothalamic, cortical, and brainstem nuclei in response to fasting and refeeding in male mice. *Endocrinology* 155: 840–853. doi:10.1210/en.2013-1831

Yen HH, Roseberry AG (2015) Decreased consumption of rewarding sucrose solutions after injection of melanocortins into the ventral tegmental area of rats. *Psychopharmacology* 232: 285–294. doi:10.1007/s00213-014-3663-6

Zhang X, van den Pol AN (2017) Rapid binge-like eating and body weight gain driven by zona incerta GABA neuron activation. *Science* 356: 853–859. doi:10.1126/science.aam7100